# Experimental and theoretical confirmation of Bloch-mode light propagation in planar photonic crystal waveguides

Marko Lončar[a)]
*Department of Electrical Engineering, California Institute of Technology, Pasadena, California 91125*

Dušan Nedeljković and Thomas P. Pearsall
*Centre Européen de Recherche de Fontainebleau, Corning, SA 77210 Avon, France*

Jelena Vučković and Axel Scherer
*Department of Electrical Engineering, California Institute of Technology, Pasadena, California 91125*

Sergey Kuchinsky
*Corning Scientific Center, 199034 St. Petersburg, Russia*

Douglas C. Allan
*SP-FR-05, Corning Incorporated, Corning, New York 14831*

(Received 11 July 2001; accepted for publication 14 December 2001)

The dispersion diagram of the leaky modes in the planar photonic crystal waveguide is experimentally obtained for the wavelengths from 1440 to 1590 nm. A small stop band, around wavelength 1500 nm, is detected. The experimentally obtained results are in very good agreement with our three-dimensional finite difference time domain calculations. Propagation losses of the leaky modes are estimated and we have found that they decrease as we approach the ministop band. © *2002 American Institute of Physics.* [DOI: 10.1063/1.1452791]

In recent years, photonic crystals[1] have attracted a lot of research attention due to their properties to control the flow of light on a very small length scale. Planar photonic crystals (PPC)[2] represent particularly promising structures for integrated optics since their planar fabrication allows the use of conventional microelectronics patterning techniques.

PPC waveguides, formed by changing the properties of one or more rows of holes in the PPC lattice, are a very active area of research.[3–13] In our previous publication,[8] we have reported that it is possible to guide the light around 60° bends in such a structure. We have also reported that in certain cases significant vertical losses are observed. Those losses could be attributed to the leaky modes of the waveguide. In this work we have experimentally mapped the dispersion diagram of the leaky modes in the wavelength range $\lambda \in (1440, 1590\ \text{nm})$. The results are in very good agreement with our three-dimensional finite difference time domain (3D FDTD) calculations.

The structure that we are interested in is a silicon slab, suspended in air and perforated with a 2D triangular lattice of holes with radius $r \approx 0.4a$, where $a$ is the periodicity of the lattice. The waveguide is defined as a row of missing holes in this triangular lattice PPC (Fig. 1). The geometry of fabricated structure is $a = 530$ nm, $r = 208$ nm, and $t = 300$ nm, where $t$ is the thickness of the slab. We have published the details of the fabrication procedure in our earlier publication.[5] The measurement setup that we used to characterize these waveguides is shown in Fig. 1. Butt coupling of a single-mode fiber was used to introduce light from a tunable semiconductor diode laser into the PPC waveguide. Waveguiding performance was observed using an infrared television camera positioned in the plane perpendicular to the sample in order to observe the light scattered in the vertical direction.

The structure that we have tested in our experiment was a single line defect (SLD) waveguide with a single defect cavity in the middle (Fig. 1). In Fig. 2 we show the pattern of light coupled out of the top surface of the waveguide structure and detected by the camera. At nearly every wavelength, a clear periodic intensity modulation can be seen along the waveguide direction. It should be noted, however, that at 1495 and 1505 nm this modulation intensity has nearly disappeared. It can further be seen that the spatial periodicity of this modulation grows shorter as the difference between the wavelength and 1500 nm grows larger, in *either direction of the wavelength*. In order to better understand these results, and to extract information on the spatial periodicity of the modulation pattern (that is propagation constant $\beta$), we have analyzed our experimental results using a fast Fourier transform (FFT).

The results of the FFT analysis of the experimental re-

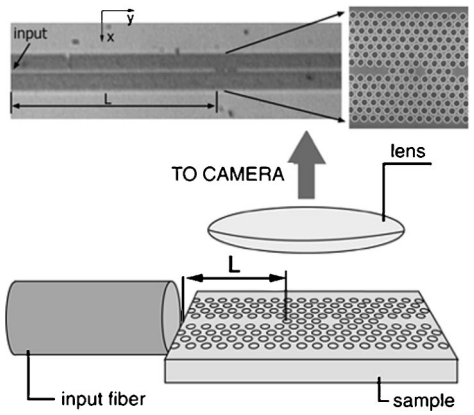


FIG. 1. Experimental setup used in the experiment. $L \approx 122\ \mu$m.

[a)]Electronic mail: loncar@its.caltech.edu

 

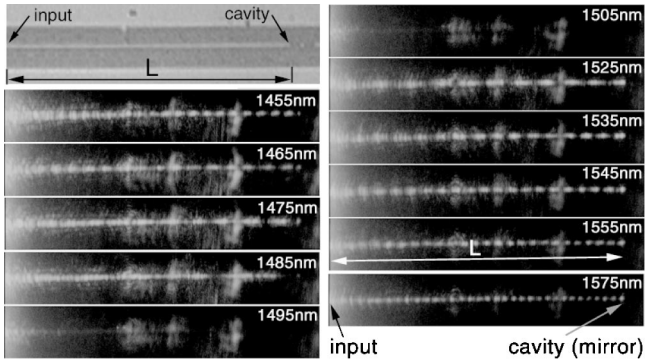


FIG. 2. Wavelength dependence of the signal scattered in the vertical direction, detected by the camera. Periodic intensity modulation can be observed for all wavelengths except for $\lambda \in (1490,1510\ \text{nm})$. Periodicity of this modulation grows shorter as the difference between the wavelength and 1500 nm grows larger, in either direction of the wavelength. Optical microscope image of the structure is also shown.

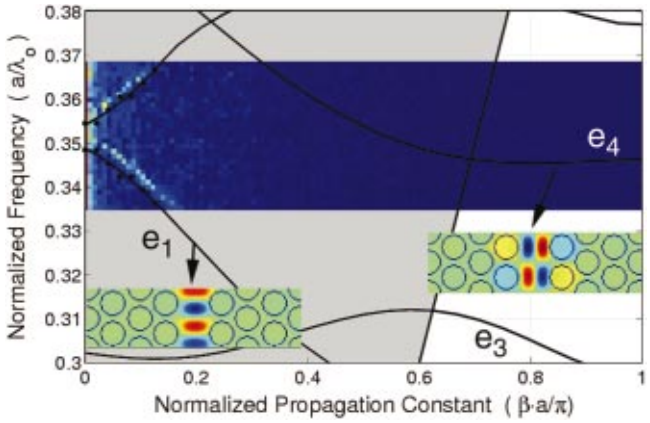


FIG. 3. (Color) Experimentally mapped dispersion diagram of the leaky TE-like modes supported in the waveguide (blue region), overlaid onto the calculated diagram (black solid lines). Insets show mode profiles ($B_z$) for two modes of interest. Light line is represented by the straight solid line, and leaky-modes region in light-gray color.

sults are overlaid onto calculated theoretical results and are presented in Fig. 3. One unit cell of the waveguide, with Bloch boundary conditions applied in the direction of propagation ($y$-axis), was modeled in order to obtain the dispersion diagram.[5] The region shown in blue in Fig. 3 is the result of the FFT of the line scans along the patterns shown in Fig. 2. The normalized propagation constants detected from the line scans are represented by light blue dots, for each normalized frequency. It can be seen that our experimental results are in a very good agreement with the 3D FDTD simulations. The slight shift of the experimental results towards the higher frequencies can be attributed to the difference between the refractive index of Si used in simulation ($n_{Si}=3.5$) and the refractive index of Si slab used in experiment, fabrication tolerances, and the resolution of the FDTD algorithm ($a=20$ computational points). Experimental results also show the presence of a small stop band around $a/\lambda=0.353$, as predicted by 3D FDTD analysis.[6] Our experimental results can now be explained in the following way. Light from the tunable laser source is coupled to leaky $e1$ mode of the waveguide, and as it propagates towards the single defect cavity it radiates energy in the vertical direction. The light in the frequency range of our laser $[a/\lambda \in (0.333,0.368)]$ cannot couple to the mode of single defect cavity located at frequency $a/\lambda=0.326$. Therefore, the light is reflected back and interferes with the forward-propagating light forming the standing wave pattern observed in Fig. 2. The cleaved input facet and the single defect cavity act as mirrors, and light coupled to the leaky modes of the waveguide resonates between them.

It is interesting to note that the same pattern as the one in Fig. 2 was observed between the input facet and the 60° bend during characterization of the SLD waveguide with $60^o$ bend in it. That indicates that in this particular design with relatively big holes, transmission around the corner is rather low for the propagating leaky modes, and the most of the light is reflected back at the bend.

In order to support our hypothesis that the signal detected by the camera is due to coupling to leaky modes, we have numerically analyzed waveguide section formed between two PPC mirrors [Fig. 4(a)]. The structure was excited using dipole sources of fixed frequency. Choosing the symmetry of the dipole sources we were able to excite only the leaky modes ($e1$). Due to the memory limitations of our computers, the length of the waveguide section was chosen to be $40.5a$ ($a=12$ points in 3D FDTD algorithm) instead of the $\approx 230a$, as it was in our experiment. In order to make calculations easier, the waveguide section was also closed with PPC at the both sides. The results are shown in Fig. 4(b) that shows profiles of the $P_z$ component of the Poynting vector in case when leaky modes were excited at three different frequencies. Periodic intensity modulation can be seen. The periodicity of this standing wave pattern has the same trend with respect to the frequency as in the experi-

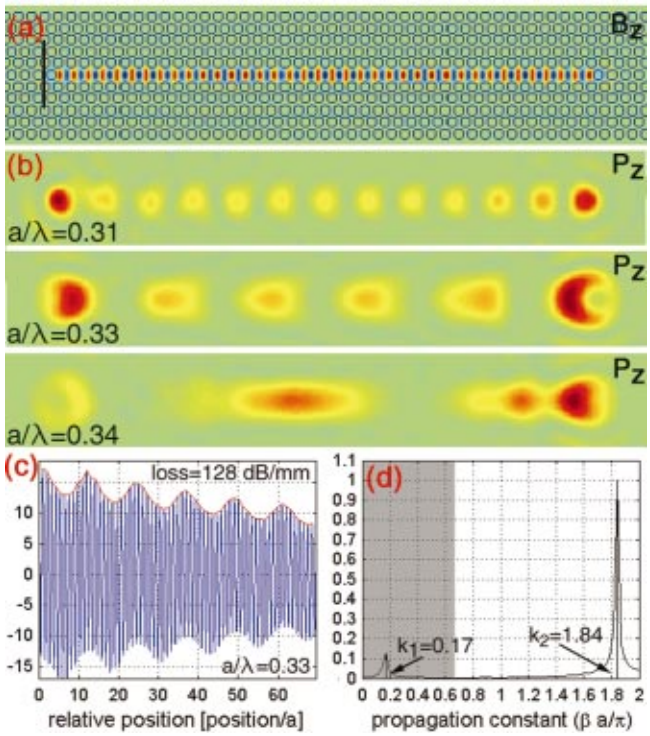


FIG. 4. (Color) (a) $B_z$ at the middle of the slab in case of a leaky mode excited in the waveguide. Position of the dipole sources is indicated by the line. (b) $P_z$ component of the Poynting vector, at a distance of about 1 $\mu$m from the top surface of the structure, shown for three different frequencies. (c) Profile of $B_z$ component taken at the center of the waveguide. Beating between two Bloch components and signal attenuation along the waveguide can be seen. (d) Spatial frequency spectrum of the signal shown in (c). Most of the mode energy is stored in the component at $k_2$. Light cone for $a/\lambda=0.33$ is represented in gray color.

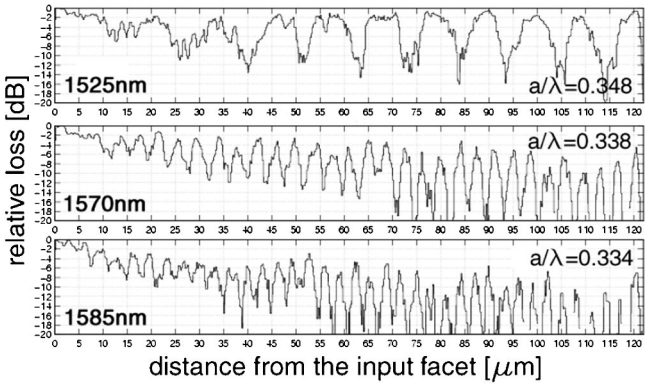


FIG. 5. Light intensity in the waveguide normalized to the intensity at the input (experimental results). Radiation losses can be seen to increase as the wavelength departs from the ministop band centered around 1500 nm.

ment: it becomes longer as the frequency approaches the ministop band. It is important to say that this standing wave pattern was detected at a distance of about 1 $\mu$m from the surface of the sample. This is again in an excellent agreement with the experiment, where the standing wave pattern was observed above the sample, i.e., at different focal distance from the one used to image the surface of the sample.

Because of the discrete translational symmetry of the PPC waveguide in $y$-axis direction, field components of each waveguide mode can be expressed as

$$B(x,y,z)=u(x,y,z)e^{i\beta y}=\sum_K U_K(x,z)e^{i(K+\beta)y}, \qquad (1)$$

$[u(x,y,z)=u(x,y+a,z)]$. $B(x,y,z)$ is one of three **B** field components, $\beta$ is Bloch wave vector limited to range $\beta\in(-\pi/a,\pi/a)$, and $K$ is reciprocal space lattice vector ($K=0,\pm 2\pi/a,\ldots$). In order to account for the losses due to radiation in the vertical direction in the case of leaky modes, Eq. (1) should be written as[14]

$$B(x,y,z)=u(x,y,z)e^{i\beta y}e^{-\alpha y}, \qquad (2)$$

where $\alpha$ is the propagation loss parameter. From Eq. (1) it follows that, in general case, each mode supported in the waveguide [defined as a single $(\beta,a/\lambda)$ point on the dispersion diagram shown in Fig. 3] is a *composite* mode made up of many Bloch components that are coupled by photonic crystal. When $\beta$ is close to zero and $a/\lambda\in(0.33,0.37)$ Bloch component for $K=0$ lies above the light line and can radiate energy in the vertical direction, while components for $K=N2\pi/a,(N=1,2,\ldots)$ are located below the light line and should not be lossy. However, they are coupled to the lossy component at $K=0$ by the PPC, and therefore will lose energy by coupling to that component. Ratio of energy stored in Bloch component for $K=0$ and energy stored in all other components will determine the losses of the whole *composite* mode defined in Eq. (2). In order to explore this loss mechanism in more details, we have modeled long waveguides ($75a$ long, $a=18$ points) using distributed 3D FDTD code. Figure 4(c) shows the intensity of $B_z$ component along the center of the waveguide, when $a/\lambda=0.33$. It can be seen that intensity of the field decreases as we move away from the input of the waveguide, yielding the losses of $\approx 128$ dB/mm. The beating between different Bloch components present in this mode is also apparent. Figure 4(d) shows the FFT of the line scan shown in Fig. 4(c). Only two spatial frequencies, located at $k_1=0.17\pi/a$ and $k_2=1.84\pi/a$, are detected in this case, and the amplitude of component $k_2$ is almost ten times bigger than the amplitude of $k_1$. Having in mind the resolution of our FFT ($0.014\pi/a$) we can write that $k_2=2\pi/a-k_1$. Finally, we can conclude that our leaky mode of interest consists only of Bloch components at $K=0$ and $K=2\pi/a$ and that more than 90% of its energy is stored in the component at $K=2\pi/a$. Because of that, the overall losses of the mode will be smaller than it would be expected having in mind only its ''distance'' from the light line. We have used distributed 3D FDTD code to estimate these losses, and we have found that losses become smaller as we approach the mini stop bend at $\beta=0$. We have attributed this to the reduction of the ratio of energy stored in Bloch components at $K=0$ and $K=2\pi/a$. However, this issue needs to be investigated in more detail.

Figure 5 shows normalized light intensity (in decibels) in the waveguide as a function of position along the waveguide, obtained from experimental results shown in Fig. 2. It can be observed that the signal detected at the end of the waveguide is stronger when the frequency is closer to the ministop band, that is that the losses are growing smaller as we approach the ministop bend. This experimental trend agrees well with 3D FDTD results.

In conclusion, we have demonstrated an equilibrium propagating mode of a photonic crystal waveguide that is a Bloch mode consisting of guided and radiative components. The radiative component, responsible for all the propagation losses has been experimentally and theoretically identified. Transmission losses of the leaky mode were estimated and it was observed that losses become smaller as we approach the ministop band. We have explained the origin of this loss reduction and have attributed it to the ratio of energy stored in radiative and guided Bloch component.

The authors would like to thank Tom Baehr-Jones from Simulant Inc. for distributed 3D FDTD code, and Sean M. Spillane and Professor Kerry J. Vahala's group at Caltech for making their computer cluster available to them.

[1] E. Yablonovitch, Phys. Rev. Lett. **58**, 2059 (1987).
[2] T. F. Krauss, R. M. De La Rue, and S. Brand, Nature (London) **383**, 692 (1996).
[3] A. Chutinan and S. Noda, Phys. Rev. B **62**, 4488 (2000).
[4] S. G. Johnson, P. R. Villeneuve, S. H. Fan, and J. D. Joannopoulos, Phys. Rev. B **62**, 8212 (2000).
[5] M. Lončar, T. Doll, J. Vučković, and A. Scherer, J. Lightwave Technol. **18**, 1402 (2000).
[6] M. Lončar, J. Vučković, and A. Scherer, J. Opt. Soc. Am. B **18**, 1362 (2001).
[7] T. Baba, N. Fukaya, and J. Yonekura, Electron. Lett. **35**, 654 (1999).
[8] M. Lončar, D. Nedeljković, T. Doll, J. Vučković, A. Scherer, and T. P. Pearsall, Appl. Phys. Lett. **77**, 1937 (2000).
[9] E. Chow, S. Y. Lin, J. R. Wendt, S. G. Johnson, and J. D. Joannopoulos, Opt. Lett. **26**, 286 (2001).
[10] T. Baba, N. Fukaya, and A. Motegi, Electron. Lett. **37**, 761 (2001).
[11] S. Olivier, M. Rattier, H. Benisty, C. Weisbuch, C. J. M. Smith, R. M. De La Rue, T. F. Krauss, U. Oesterle, and R. Houdré, Phys. Rev. B **63**, 113311 (2001).
[12] X. Letartre, C. Seassal, C. Grillet, P. Rojo-Romeo, P. Viktorovitch, M. Le Vassor d'Yerville, D. Casagne, and C. Jouanin, Appl. Phys. Lett. **79**, 2312 (2001).
[13] M. Notomi, A. Shinya, K. Yamada, J. Takahashi, C. Takahashi, and I. Yokohama, Electron. Lett. **37**, 293 (2001).
[14] J. Vučković, M. Lončar, and A. Scherer, IEEE J. Quantum Electron. **36**, 1131 (2000).